SOILS, SEC # • RESEARCH ARTICLE

Changes in micro-fabric and re-distribution of Fe and Mn with nodule formation in a floodplain soil

Péter Sipos[1] • Réka Balázs[1] • Gábor Bozsó[2] • Tibor Németh[1]

[1]Institute for Geological and Geochemical Research, Research Centre for Astronomy and Earth Sciences, Hungarian Academy of Sciences, H1112 Budapest, Budaörsi út 45., Hungary

[2]Department of Mineralogy, Geochemistry and Petrology, University of Szeged, H6722 Szeged, Egyetem utca 2., Hungary

✉ Péter Sipos

sipos.peter@csfk.mta.hu

Phone: +3613092600

Abstract

Purpose. Ferromanganese nodules are common features in aquic soils of the temperate climate. Although they are intensively studied due to their pedogenic significance, there is a lack of knowledge on the relationship between their micro-fabric and distribution of their major chemical components. Our aim was to fill this gap and to relate these characteristics to the different stages of the nodule development in the soil.

Materials and methods. To fulfil our aims, ferromanganese nodules from a Gleyic Fluvisol profile was separated in which nodules with strongly varying appearance and fabric are present in a wide depth interval, so they are expected to represent the different stages of nodule formation. Micro-chemical analyses were carried out on the polished surface of 28 nodules. Micro-X-Ray fluorescence spectrometry was used to produce Fe and Mn elemental maps of the whole nodules as well as line scan analyses along perpendicular cross sections. Additionally, the spatial distribution and major element associations of Fe and Mn within the individual nodules were studied by point analyses at 775 spots by electron microprobe analysis.

Results and discussion. Typic and concentric nodules in the soil exhibited both similar (presence of outer coating band) and different (undifferentiated and banded interior, respectively) characteristics in their micro-fabric. These were related to the rate of hydromorphism in the soil which was found to determinate the major processes (accretion vs. impregnation) forming the fabric of the nodules. The following stages of the nodule development were distinguished: 1) cementation; 2) formation of outer band; 3) re-arrangement and slow impregnation of nodules' interior; 4) fast impregnation of the interior and exfoliation of outer band. We found that separation of Fe and Mn is characteristic of each stage of nodule formation. However, as long as spatial segregation occurs in the first stages, displacement of Mn by Fe is rather typical later.

Conclusions. Fabric and appearance of nodules form by varying rate and dominance of accretion and impregnation relatively slowly. However, distribution pattern of Fe and Mn within the nodules may exhibit much faster changes simultaneously. Complex micro-chemical analyses support a powerful tool to follow such changes and to get a deeper insight into the genesis of ferromanganese nodules.

Keywords Concentric nodules • Fe and Mn distribution • Micro-fabric • Microprobe • Micro-XRF • Typic nodules

1 Introduction

Ferromanganese nodules in which Fe and Mn are concentrated relatively to the matrix are general phenomena in aquic soils of temperate climate. In such environment, these elements are mobilized by reduction and afterwards they are concentrated in various forms in oxidizing conditions (Schwertmann and Fanning 1976). Their compounds to be expected in these soils may show strong separation due to the differences in their solubility and that in the oxidation of Fe and Mn under soil Eh-pH conditions occurring naturally (Krauskopf 1957). This marked separation was also observed in nodules by their first electron microscopy studies, and it was attributed to the alternation of Eh in the soil (Cescas et al. 1970). Later, the Fe and/or Mn enrichment within the nodules were related to their mineralogy (Pawluk and Dumanski 1973), relative age (Schwertmann and Fanning 1976), colour (Dawson et al. 1985), size and structure (Sanz et al. 1996), shape (White and Dixon 1996) and to the water logging of the soil (Cornu et al. 2005). The detailed model of nodule formation and that of the Fe and Mn distribution within was described by White and Dixon (1996) first. Accordingly, alternating Eh conditions in soil may result in different redox potential in the soil solution and at the surface of the nodules even at the same time. Consequently, dissolution and/or precipitation of Fe and/or Mn oxides, as well as diffusion of Fe and/or Mn ions may be proceeded within the nodules resulting in diverse distribution pattern for the metals in question. Moreover, Palumbo et al. (2001) observed the presence of Mn oxide precipitates in the fractures and pores of several nodule types suggesting that the internal circulation of pore water and the precipitation of oxides continue after the nodule formation, as well. The high concentration of reducible material in a compact form and the relatively low porosity result in a kinetically resistant formation against reduction for nodules so they can be preserved also at oxidizing conditions.

Micro-analytical study of ferromanganese nodules is of decades-long tradition. It was originally based on the study of the distribution of major chemical elements within single nodules. Most recent studies, however, include identification of specific minerals (Timofeeva et al., 2014), quantitative elemental analyses (Cornu et al. 2005) and specification of the micro-fabric of ferromanganese nodules (Gasparatos et al. 2005). The distribution characteristics of Fe and Mn within different types of nodules were also described and it was related to the different mode of their formation (Zhang and Karathanasis 1997; Palumbo et al., 2001). It was found that different types of nodules reflect different pedogenic features which can describe the course of soil formation (Hickey et al., 2008). Consequently, study of the differences in Fe and Mn concentration and distribution in nodules may reveal a detailed history of the redox characteristics in the soil micro-environment. In spite of this, the micro-fabric of nodules as related to the distribution of Fe and Mn within is only rarely studied (Gasparatos

et al. 2005). Moreover, elemental maps and line scan analyses have been generally carried out to study Fe and Mn distribution in the nodules but no large number of point analyses. Albeit they can be useful to specify the metal distribution at micro-scale and nodule development can be outlined in more details. For example, development of nodules with different appearance and fabric at low distance within a given soil profile can be described using combination of such analyses. Our aims were (1) to study the differences in micro-fabric within individual nodules representing different types; (2) to relate their micro-fabric to the stages of nodule development; and (3) to study the relation of distribution of Fe and Mn to the micro-fabric. For this study, a floodplain soil was chosen in which several types of nodules appear in a wide depth interval representing different stages of nodule development.

2 Materials and methods

2.1 Soil samples and their preparation for analyses

The studied soil-sediment profile was sampled on a floodplain meadow (slope gradient <5%) with grassy vegetation, 200 m away from the river Ipoly at Ipolyszög, North Hungary. The climate is humid continental with average annual temperature of 9.5°C (20.5°C in summer and -2.0°C in winter). The number of days when the temperature does not exceed 0°C is less than 30 annually. The annual average precipitation is 610 mm (half of it in the summer period). The WRB soil type is Gleyic Fluvisol (Calcaric). The soil formed on Holocene alluvial clay. The profile was sampled down to 250 cm continuously. Its most important physico-chemical properties are shown in Table 1.

The soil pH shows a slight increase downwards: it is neutral in the upper (above 60 cm) and slightly alkaline in the lower layers of the profile. In close relation to that calcite appears in the profile below 90 cm depth. The total organic carbon content of the soil decreases downwards from the maximum value of 3.14% and it is still relatively high (0.47%) down to 120 cm. The soil texture is clay with nearly steady and high clay content in the whole profile (661 ± 56 g/kg clay). The major clay mineral species are in the order of dominance: smectite >> illite > kaolinite. More detailed mineralogical characterization of the profile can be found in the paper by Sipos et al. (2011). The total Fe content of the soil varies between 4.39 and 5.41% with a slight enrichment in the layers between 40 and 60 cm, as well as between 180 and 230 cm. In contrast, total Mn content of the samples are between 333 and 1529 mg/kg, and it shows one maximum between 120 and 150 cm, and also significant depletion below 180 cm. Oxalate and dithionite soluble Fe show decrease downwards but that of Mn varies parallel to the total Mn content.

Redoximorphic features appear below 20 cm in the profile. Redox concentrations in form of Fe/Mn masses and nodules are characteristic between 20 and 180 cm, with the highest frequency and size for nodules between 60 and 90 cm. Below this layer, Fe/Mn depletion spots also appear down to 230 cm. Additionally, carbonate mottles can be observed between 90 and 180 cm. Below 230 cm, Fe/Mn depletion matrix is characteristic. Microscopic study of Sipos et al. (2009) on pedofeatures from this profile showed the presence of goethite pseudomorphs after amphiboles in the layer between 60 and 120 cm, which may have served as the source of Fe in this case.

The collected samples were air dried. Total soil samples were grounded to fine powder (<10 μm) in an agate mortar for chemical analyses. Separation of the clay fractions (<2 μm) were carried out by sedimentation in aqueous suspension. Ferromanganese nodules were separated following the instructions of Gasparatos et al. (2005). For electron microprobe and micro-XRF analyses, 6-8 ferromanganese nodules from each layer were set into resin, cut to show a cross section and micro-polished. The polished surfaces were also coated by carbon for electron microprobe analyses.

2.2 Soil analysis and analytical methods

Soil pH was analysed in 1:2.5 soil:distilled water suspension. The total organic carbon content of the samples was determined by a Tekmar-Dohrmann Apollo 9000N TOC analyser instrument. Particle size distribution of the samples was studied by a Fritsch Analysette Microtech A22 laser diffraction analyser. The soil samples, their clay fractions and the separated ferromanganese nodules were studied for their mineralogy using a Philips PW1710 X-Ray diffractometer from the powdered materials. Total Fe and Mn content of the bulk samples were analysed by a Philips PW1410 X-Ray fluorescence spectrometer from pressed powder pellets. Also bulk soil samples from selected layers were subjected to sodium-dithionite and ammonium-oxalate dissolution according to the methods of USDA (Burt 2004). Concentrations of Fe and Mn in the extractions were analysed by a Perkin Elmer AAnalyst 300 atomic absorption spectrometer (see details in Sipos et al. 2011).

Micro-chemical analyses were carried out on the polished surface of the ferromanganese nodules. Altogether, 28 nodules were analysed by such methods. Micro-X-Ray fluorescence spectrometry was used to analyse the distribution of Fe and Mn within the different types of ferromanganese precipitations using a Horiba Jobin Yvon XGT 5000 spectrometer. Distribution maps and line scan analyses along perpendicular cross sections of the whole nodules were carried out. The X-Ray source was a Rh-tube with 30kV excitation voltage, 1mA anode current and 10 μm spot size. Elemental distribution maps were recorded in a frame size of 3.072×3.072 mm. Each frame was scanned 10 times with a live time of 50 s and they consisted of 512 pixels with the size of 6×6

μm. Spatial distribution of the major chemical elements among and within the phases composing the nodules was studied by point analyses in the 28 nodules at 775 spots by a JEOL Superprobe JCXA-733 type electron microprobe equipped with an INCA Energy 200 energy dispersive spectrometer. An acceleration voltage of 20 kV, a probe current of 3 nA and a count time between 10 and 30 s was used for the analyses. The diameter of the electron beam used for the micro-chemical analyses was 1 μm. The fabric of the ferromanganese nodules was studied by analysing the backscattered electron images of the polished surfaces.

3 Results

3.1 Ferromanganese nodule types

Nodules were observed in a wide depth-interval (between 20 and 180 cm) in the studied profile. The main zone of their in situ formation is between 60 and 90 cm based on their highest frequency and largest size in the profile, whereas only their fragments could be found below 150 cm (more details in Sipos et al. 2009). The nodules showed large variation in their appearance and (micro-) fabric with depth. They could be classified in two major types as follows.

Typic nodules. Nodules composed of coarse soil particles cemented by Fe and Mn oxides at different rate can be observed in each layer where any type of nodules is characteristic in the profile. These nodules are of irregular shape and diffuse edge; their size rarely exceeds 1 mm. Their compactness increases with depth: the coarse soil particles are cemented together by the Fe and Mn oxides only sporadically in the upper layers resulting in a gefuric distribution pattern, whereas the appearance of a porphyric-like character was observed in the lower ones in this kind of nodules (Fig. 1). Large cracks and voids (up to several tens of μm) with vughy microstructure were also observed in the latter ones with decreasing size and frequency with depth. The higher the ratio of the Fe and Mn oxides to the cemented coarse soil particles the higher the compaction of the nodules. This can be due to both matrix and intrusive features, like impregnation of the non-oxide soil material as well as filling up of voids, coating of their walls, coarse particles and even the whole nodules, respectively. The most conspicuous one of these features are the coating bands of Fe and Mn oxides of several generations (Fig. 1). The thickness of such single bands may be as large as 20 μm, whereas that of the whole coating band varies between a few tens of μm up to 200 μm. The coating band forming on the surface of the nodules is generally more compacted than the nodule's interior (primarily its outer 20-30 μm) in spite of the presence of large voids. Although their formation could be observed also in the upper layers partly complete coating band on the nodules were found below 60 cm only. When it is present at least partly the shape of the nodule tends to be rounded but still with diffuse edges

both at the outer and the inner edges. The microstructure of the interior of such nodules is still dominated by the irregular smooth vughs, whereas loosely stacked particles and strongly cemented parts are present alike. However, when a complete outer coating band is present, the interior of such nodules show much higher cementation than that of those with a partial coating band although large voids are still present (up to 50-100 μm). All of these nodules mentioned above can be considered as typic nodules (Stoops, 2003). They are the only nodule type in the layer between 20 and 60 cm with increasing frequency downwards and can be also found in the lower layers but only subordinately as compared to concentric ones.

Concentric nodules. They appear in the layer between 60 and 150 cm in the profile with the largest size and highest frequency in its upper 30 cm. Here, nodules of relatively large size (generally around 2 mm) and composing of several thin concentric bands are characteristic (Fig. 2). Their shape is rounded; their edges are strongly diffuse but can be slightly sharp sporadically primarily below 90 cm. A similar outer coating band to those characteristic of some typic nodules can be also observed in this case. However, this band can be exfoliated partly as suggested by micro-bands reaching the broken edges. Within this coating band several other concentric bands were developed separated by large cracks and series of vughs which tend to follow the shape of the outer coating band. These bands are cemented at similar rate as the outer band is, and their thickness shows large variation between 10 and 100 μm generally. The innermost part of such nodules shows the lowest compactness. Also in the layer between 60 and 90 cm, nodules with sharp edges and with a large void (size of 500-800 μm) in their centre are present, too. Their shape is rounded which can be related to the significant loss of the outer coating band. It is present only as fragments in this case. A thin (a few μm) coating composed of silicates may be present where the outer coating band is absent (Fig. 2). Sharp edge of the central void suggests that the geode-like structure can be due to the dissolution (and re-arrangement) of a former core. Around this void, one large band is present generally with a thickness of 3-600 μm. It has a micro-fabric similar to that of the inner bands of the other concentric nodules. These are strongly cemented but large voids can be still frequent within them. They are dominantly composed of silicates impregnated by Fe oxides and of void-filling “clear” Mn oxides (e.g. Fe and other silicate-forming major elements could not be detected). Below 90 cm, concentric nodules with incomplete outer coating band and a few thick inner bands are dominant (Fig. 2). Generally, the massive (up to 500 μm of thickness) outer coating band has been exfoliated partially and show lower compactness than the inner bands. The edge of such nodules is rather sharp and it is also characteristic of the inner surface of the outer coating band if it is present. The inner bands are up to 300 μm thick and are separated by thin cracks and series of relatively large vughs. The innermost parts of these nodules are also strongly

impregnated suggesting cracks and voids are mostly filled up with the cementing material in the nodules' interior. The micro-fabric of the inner bands is mostly inhomogeneous and undifferentiated but banded and coated structures may appear sometimes with relatively large size (up to several hundreds of μm) consisting of alternating silicate-rich and Fe or Mn oxide-rich bands. Nodules composed of an outer coating band and varying number of concentric inner bands can be all considered as concentric nodules (Stoops, 2003). They are the dominant forms below 60 cm depth and show higher compactness in their interior than the typic nodules.

3.2 Distribution of Fe and Mn within the nodules

Within typic nodules of gefuric microstructure, Fe shows patchy whereas Mn does rather uniform distribution. Additionally, a slight enrichment at the nodules' edge for both metals was also observed which can be related to the formation of coating bands. Point analyses showed the close association of both Fe and Mn oxides with silicates, e.g. these phases could not be separated using an electron beam of 1 μm diameter. The only exception is the rare presence of "clear" Mn oxides in the interior part of such nodules (Fig. 3). As the rate of the cementation increases in the typic nodules the enrichment of Fe at the edges and that of the Mn in the interior is getting characteristic more and more. Interestingly, it is not strictly related to the microstructure of the nodules, although it can be related to the (start of the) formation of a coating band. For example, Fe enrichment at the nodules' edge could be developed without any visible presence of a coating band. Additionally, when this latter is present its thickness may be significantly different from that of the band characterized by the highest Fe enrichment. This was also supported both by line scan and point analyses. These latter showed that the 50-100 μm thick edge of the nodules are composed of the mixture of "clear" Fe oxides and Fe oxide-silicate phase associations free of Mn. This latter metal was only detected in the internal parts of the coating band although its concentration never reached that of Fe at any of the analysed points. Additionally, "clear" Mn oxides were found only rarely and within the coating band exceptionally. Such band with Fe enrichment is characteristic of the porphyric typic nodules rather. Contrarily those of gefuric microstructure could be characterized by Mn enrichment with "clear" Mn oxides even at the nodules edge and very close to "clear" Fe oxide precipitations (at a few μm distance) (Fig. 4).

Distribution of Fe and Mn in the concentric nodules shows large similarities to that of the compact typic nodules with outer coating band. It is expressed by the same pattern for Fe and Mn in the coating band, e.g. Fe enrichment with no detectable Mn in the outer edge of this band, and presence of tiny "clear" Mn oxides in its internal part. Iron is generally closely associated to silicates there. In the interior of such nodules, quasi-

concentric bands with Fe enrichment were observed both by elemental maps and line scan analyses. Although Mn may be also settled in bands there it shows rather patchy distribution (Fig. 5). The ratio of Fe to Mn increases outwards such a way that concentration of Fe does not exceed that of Mn necessarily. This change in the Fe/Mn ratio may be repeated several times even within one thick inner band (Fig. 6). Association of Mn and Fe oxides to silicates is still very close; however, "clear" Mn and even Fe oxides may appear as void or crack fillings with maximum size of 10 μm. The innermost part of these nodules is composed of closely associated Fe oxides and silicates, as well as "clear" Mn oxides as crack and void fillings. As their compactness increases ratio of Fe to other major components increases, as well. Interestingly, exposed inner surfaces after the loss of the outer coating band also show Fe enrichment at their edges as shown by elemental maps. However, it is not as characteristic as in the case of the outer coating band. Additionally, it is often expressed by the increase of the Fe content within the phase-association of Fe-Mn oxides and silicates sometimes without Fe concentrations exceeding that of Mn.

4 Discussion

Saturation of sufficiently long duration to develop anaerobic soil, sufficient organic carbon and warm-enough soil temperatures to support microbial activity and adequate supplies of Fe and Mn are necessary for the development of redoximorphic features in soils (D'Amore et al. 2004). Their presence (both depletions and concentrations) in the studied profile provides the best evidence that all these conditions have been existed there. Moreover, soil physico-chemical and mineralogical properties, as well as pedogenic conditions at the profile's location suggest that recent formation of such pedofeatures can be also expected.

4.1 Nodule development

The first stage of the nodule formation is the cementation of coarse soil particles by Fe and Mn oxides to form aggregates with irregular shape. Chiang et al. (1997) showed that weathered coarse particles within a clayey soil matrix with their relatively large porosity are ideal for Fe and Mn oxidation and concentration to occur promoting the formation of ferromanganese nodules. Near to the surface, however, sufficiently long periods of water saturation are generally not fulfilled. Additionally, high organic matter content of the surface soils inhibits the crystallization of Fe and Mn oxides and hereby the stabilization and growth of nodules (Jien et al. 2010). Therefore, typic nodules with gefuric fabric could only be developed in such layers. As the effect of hydromorphism increases downwards the rate of cementation increases as well in the nodules. This is

accompanied through the complete coating of coarse particles and gradual filling up of voids through the formation of several micro-bands. This suggests their formation in waves during alternating wet and dry periods (Gasparatos et al. 2005). Parallel to that, aggregates start to be coated by Fe and Mn oxides contributing to the development of a compact outer coating band for the nodules. This can be considered as the second stage of nodule development. The presence of the outer coating band is a general phenomenon for ferromanganese nodules (see White and Dixon 1996 and references therein). They are responsible for the development of the rounded shape of the nodules. Additionally, they provide a strong physical protection for nodules against decomposition and also a unique micro-chemical environment resulting in different micro-fabric for the external and internal parts of the nodules. We found that the micro-fabric of the outer coating band shows large similarities to that of the well-compacted aggregates suggesting that it forms not only through periodic coating of the nodule by Fe and Mn oxides but through an accretion process where coated soil particles are cemented to the surface of the nodules. Based on selective chemical extraction of Fe in water-logged soils, Jien et al. (2010) also found that large nodules may have formed from the smaller ones gradually by accretion through poorly crystalline Fe oxides. This also results that the development of the outer band is not uniform which is supported by the general observation that it shows high variance in its thickness and cementation. Nodules at the above developmental stages always exhibit diffuse boundary which is often considered to be indicative of contemporary development (Constantini and Priori 2007).

The nodules' interior within the outer coating band may be cemented in a varying degree showing an increase in the profile downwards. In the third stage of the nodule development, the re-arrangement of the cracks and voids accompanied with the Fe and Mn oxide precipitation in several micro-bands is proceeded. They show, however, significantly different micro-fabric than outer bands do, which indicates that the major processes of their formation are impregnation and cementation. These processes result in the gradual impregnation of the nodules interior and filling up of cracks and voids, as well as in the settling of voids circularly. Although circular settling of bands are generally thought to be the result of several generations of Fe and/or Mn oxides precipitating under the influence of the periodic water-logging in soil (Gasparatos et al. 2005), this may be not the case within a compact outer band. Their formation should be a slower process than that of the outer coating band as the migration of solutions is restricted. As this process progressing, number of bands decreases with their fusion by cementation. A number of studies have shown that soil nodules are not banded or they have only an outer band around and an inner core with undifferentiated fabric (e.g. White and Dixon, 1996). Nodules with many bands were identified only later and their joint presence with non-banded nodules in the same profile was also observed

(Liu et al. 2002). Our data suggest that these types of nodules represent the different stage of their development. Their appearance in the same profile can be expected at the different layers exhibiting different degree of hydromorphism. Additionally, larger number of bands does not mean longer history of their development necessarily although it was the general opinion earlier (e.g. Cescas et al. 1970). The re-arrangement of cracks and voids and formation of concentric bands in the nodules' interior may be affected also by the presence of swelling clay minerals (smectite) in our case. They may promote the arrangement of the nodules interior within the frame of a compact outer band. Jien et al. (2010) also found that the orientation of clay minerals may play a significant role in the nodule development and clay content might be a factor influencing the size of the nodules, as well.

As the compactness of the nodules' interior reaches a similar degree to that of the outer coating band, this latter one starts to exfoliate from the internal parts gradually. This process represents the fourth stage of the nodule development and may be due to both chemical and physical processes. The former is the dissolution of the outer surface of the nodules which is suggested by the tendency of sharpening of the nodules' edges. This is characteristic primarily below 90 cm in our case. Fast variation of wetting-drying cycles (Rudeforth 1970), low water conductivity of soils (Schwertmann and Fanning 1976) and increasing duration of water saturation in the soil (White and Dixon 1996) promotes the dissolution of the cementing material and it should smooth the surface creating sharp boundaries (Vepraskas et al. 1994). The high amount of swelling clay minerals in the studied soil and the appearance of such nodules below the depth of highest hydromorphism all suggest the contribution of the processes mentioned above. As the dissolution of the nodules' surface and the cementation of their interior progresses simultaneously, the latter process together with the tension of the swelling clay minerals may also contribute to the exfoliation of the coating band. If the inner bands are exposed they may be coated by micro-bands composed primarily of silicates as shown by our data in the case of the nodules with geode structure. Earlier studies suggested (e.g. Tucker et al. 1994) that if the redoximorphic features in soils are coated by illuvial clay, they are most likely not contemporary. However, this does not always mean the nodule did not form in situ (Stolt et al. 1994). As nodules with geode-structure can be found in the same layer where a younger generation of concentric nodules exists, they may represent the relicts of a previous nodule generation formed in periods of shallower groundwater level than the present one.

4.2 Fe and Mn (re-)distribution

Iron and manganese show strong separation in their distribution within the nodules as shown still by the first electron microscope studies of nodules (Cescas et al. 1970). This separation begins in the initial stage of the nodule formation already, although both metals may enrich at the edges due to the precipitation of their oxides onto the nodules' surface. This results in the higher cementation of the edges and hereby in the formation of the outer coating band. However, as cementation progresses, Fe begins to dominate near to the surface of the nodules despite that no clear evidence for the coating band can be observed based on their micro-fabric yet. Contrarily, the interior of such nodules can be characterized by an obvious Mn-dominance besides the general presence of Fe. Jien et al. (2010) also observed that Mn tends to enrich in the inner parts of the nodules in the early stage of nodule development due to more oxidizing conditions there. This may indicate that these nodules grew when the oxidized nodule was in a soil alternately oxidized and reduced with respect to Fe but always reduced with respect to Mn (White and Dixon 1996). As the characteristic micro-fabric of the outer band develops, the separation of Fe and Mn within the nodules is getting more conspicuous. Their separation can be observed even within this band: as long as its external part can be free of Mn completely, its internal part may contain Mn as well even in form of Mn oxides free of Fe and other major elements characteristic of silicates. The close association of Fe to the latter elements is also a general phenomenon in the studied nodules. It is known that Si may affect the solubility of Fe in soils (Saleh and Jones 1984) which is supported also by Rhoton et al. (1993) who found that DCB-extractable Si inhibits the dissolution of Fe oxides in soils. These data suggest that close association of Fe and silicates may result in more stable precipitation than "clear" Fe or Mn oxides promoting their more effective preservation through the nodule development.

Dominance of Fe or Mn in certain parts of nodules is strongly affected by the hydromorphic effects in the soil. Slow and significant changes in redox condition are advantageous for the separation of these two metals. However, Eh can be significantly different in the whole soil and in the nodules interior as the latter would kinetically resists reduction because of the high concentration of reducible material in a compact form with low porosity (Huang et al. 2008). As the Eh drops the nodules' surface becomes reduced first with respect to Mn only resulting in its depletion. On the contrary, when the oxidation of the soil commences the Eh of the nodule's surface will be close to that of the soil solution. In this case the surface will be oxidizing initially with respect to Fe but not to Mn and a coating rich in Fe could form (White and Dixon 1996). Based on the above, the Eh generally do not reaches that of Mn oxidation-reduction couple in the studied profile, as no Mn oxide precipitation on the surface of nodules was found. After its dissolution, Mn may also diffuse towards the nodules' interior where redox conditions prefer its precipitation as oxides, as suggested by the presence of

"clear" Mn oxides as crack and void fillings. Such conditions may be present as long as a compact outer coating band is not formed. After that the migration of the soil solution into the nodules will be more restricted and the ratio of Fe to Mn begins to increase due to the higher supply of the former metal. In relation to that, the loose structure of the nodules interior can be explained by the low amount of cementing material (e.g. Mn supply) in the initial stage(s) of nodule formation. Schwertmann and Fanning (1976) also observed the gradual exhausting of Mn as nodule development progresses and explained by the higher Fe supply in soils as compared to that of Mn. Additionally, Mn oxides are able to oxidize Fe^{2+} and therefore influencing the site of its deposition (Golden et al. 1988). This process may also contribute to the increase in the precipitation of Fe oxides in the nodules' interior in the later stages of nodule development.

Slight separation of Fe and Mn could be observed also within the inner bands of the nodules as shown by the periodic increasing Fe/Mn ratio outwards. Such characteristics have not been observed before, as large number of point analyses has not been carried out on soil nodules either. This phenomenon can be explained by the cementation of several thin bands to form a larger one. However, they preserve their original elemental distribution characteristics meanwhile. As long as conditions for internal circulation of pore water exist, precipitation of Fe and Mn oxides continues even after the nodule formation (Palumbo et al. 2001). This may result in the formation of Fe and Mn rich bands within the nodule and also the increase of the amount of Fe in the cementing material. As the water movement is reduced later, redox potential can not be low enough for the mobilization of Fe primarily if it is coupled with low organic C levels (Rhoton et al. 1993). This may be also responsible to the gradual displacement of Mn by Fe in the nodules' interior.

5 Conclusions

Ferromanganese nodules of different types exhibit both similar (presence of outer coating band) and different (undifferentiated or banded interior) characteristics in their micro-fabric which can be primarily related to the rate of hydromorphism in the soil. As long as the major process for the development of the outer coating band is accretion and that of the inner parts are impregnation they result in significantly different micro-fabric even within an individual nodule. The actual fabric of nodules forms by varying rate and dominance of these processes relatively slowly. In close relation to the frequency and length of water-logging, the following stages of nodule development were distinguished: 1. cementation; 2. formation of outer coating band; 3. re-arrangement and slow impregnation of the nodules' interior; 4. fast impregnation of the nodules' interior and exfoliation of the outer coating band.

Separation of Fe and Mn was observed in the earliest stages of the nodule development already. With increasing rate of hydromorphism, the dominance of Mn oxides material turns to that of Fe oxides in the cementing, but this process does not proceed simultaneously in the different parts of the nodules. This latter can be related to the co-existence of numerous conditions, like differences in Fe and Mn supply, in re-dissolution of its oxides, in resistance of their phase associations and in diffusion towards the nodules interior. Separation of Fe and Mn is generally faster than the micro-textural development of the nodules so their distribution may predict textural changes, as well.

Micro-chemical analyses involving the joint study of micro-fabric and distribution of major chemical components support a powerful tool to follow their changes and to get a deeper insight into the genesis of ferromanganese nodules.

Acknowledgements This study was financially supported by the Hungarian Scientific Research Fund (OTKA K105009). Péter Sipos also thanks for the support of the János Bolyai Research Scholarship of the Hungarian Academy of Sciences.

References

Burt R (ed) (2004) Soil survey laboratory manual. Soil Survey Investigations Report No. 42. USDA Natural Resources Conservation Service

Cescas MP, Tyner EH, Harmer RS (1970) Ferromanganiferous soil concretions: A scanning electron microscope study of their micropore structures. Soil Sci Soc Am Proc 34:641-644

Chiang HC, Hseu ZY, Chen ZS (1997) Micromorphology of iron nodules in a montane Ultisol of central Taiwan. Taiwan For Sci 12:41–420

Constantini EAC, Priori S (2007) Pedogenesis of plinthite during early Pliocene in the Mediterranean environment: case study of a buried paleosol at Podere Renieri, central Italy. Catena 71:425-443

Cornu S, Deschatrettes V, Salvador-Blanes S, Clozel B, Hardy M, Branchut S, Le Forestier L (2005) Trace element accumulation in Mn-Fe-oxide nodules of a planosolic horizon. Geoderma 125:11-24

D'Amore DV, Stewart SR, Huddleston JH (2004) Saturation, reduction, and the formation of iron–manganese concretions in the Jackson-Frazier Wetland, Oregon. Soil Sci Soc Am J 68:1012–1022

Dawson, B.S.W., Fergusson, J.E., Campbell, A.S., Cutler, E.J.B., 1985. Distribution of elements in some Fe-Mn nodules and an iron-pan in some gley soils of New Zealand. Geoderma 35:127-143

Gasparatos D, Tarenidis D, Haidouti C, Oikonomou G (2005) Microscopic structure of soil Fe-Mn nodules: environmental implication. Environ Chem Lett 2:175-178

Golden DC, Dixon JB, Kanehiro Y (1993) The manganese oxide mineral, lithiophorite, in an Oxisol from Hawaii. Aust J Soil Res 31:51-66

Hickey PJ, McDaniel PA, Strawn DG (2008) Characterization of iron-manganese cemented redoximorphic aggregates on Wetland soils contaminated with mine wastes. J Environ Qual 37:2375-2385

Huang L, Hong J, Tan W, Hu H, Liu F, Wang M (2008) Characteristics of micromorphology and element distribution of iron–manganese cutans in typical soils of subtropical China. Geoderma 146:40-47

Jien SH, Hseu ZY, Chan ZS (2010) Hydropedological implications of ferromanganiferous nodules in rice-growing Plinthitic Ultisols under different moisture regimes. Soil Sci Soc Am J 74:880–891

Krauskopf KB (1957) Separation of manganese from iron in sedimentary processes. Geochim Cosmochim Acta 12:61-84

Liu F, Colombo C, Adamo P, He JZ, Violante A (2002) Trace elements in manganese-iron nodules from a Chinese Alfisol. Soil Sci Soc Am J 66:661-670

Palumbo B, Bellance A, Neri R, Roe MJ (2001) Trace metal partitioning in Fe-Mn nodules from Sicilian soils, Italy. Chem Geol 173:257-269

Pawluk S, Dumanski J (1973) Ferruginous concretions in a poorly drained soil of Alberta. Soil Sci Soc Am Proc 37:124-127

Rhoton FE, Bigham JM, Schulze DG (1993) Properties of Iron-Manganese Nodules from a Sequence of Eroded Fragipan Soils. Soil Sci Soc Am J 57:1386-1392

Rudeforth CC (1970) The micromorphology of surface water gley soils. In: Osmond DA, Bullock P (eds) Micromorphological techniques and applications. Agricultural Research Council. Soil Survey. Technical Monograph 2, Harpenden, pp 69-81

Saleh AM, Jones AA (1984) The crystallinity and surface characteristics of synthetic ferrihydrite and its relationship to kaolinite surfaces. Clay Miner 19:745-755

Sanz A, Garcia-Gonzalez MT, Vizcayno C, Rodriguez R (1996) Iron-manganese nodules in a semi-arid environment. Aust J Soil Res 34:623-634

Schwertmann U, Fanning DS (1976) Iron-manganese concretions in hydrosequences of soil in loess in Bavaria. Soil Sci Soc Am J 40:731-738

Sipos P, Németh T, May Z (2009) Vasas kiválások ásványos összetétele egy Ipoly-menti réti talajban. Agrokémia és Talajtan 58:27-44

Sipos P, Németh T, May Z, Szalai Z (2011) Accumulation of trace elements in Fe-rich nodules in a neutral-alkaline floodplain soil. Carpath J Earth Env 6/1:13-22

Stolt MH, Ogg CM, Baker JC (1994) Strongly contrasting redoximorphic patterns in Virginia Valley and Ridge paleosols. Soil Sci Soc Am J 58:477-484

Stoops G (2003) Guidelines for analysis and description of soil and regolith thin sections. Soil Sci Soc Am, Madison, WI

Timofeeva YO, Karabatsov AA, Semal' VA, Burdukovskii ML, Bondarchuk NV (2014) Iron-manganese nodules in Udepts: the dependence of the accumulation of trace elements on nodule size. Soil Sci Soc Am J 78:767-778

Tucker RJ, Drees LR, Wilding LP (1994) Signposts old and new: active and inactive redoximorphic features, and seasonal wetness in two Alfisols of the Gulf coast region of Texas, USA. In: Ringrose-Voase AJ, Humphreys GS (eds.) Soil micromorphology: studies in management and genesis. Developments in soil science, Vol. 22, Elsevier, Amsterdam, pp 99-106

Vepraskas MJ, Wilding LP, Drees LR (1994) Aquic conditions for soil taxonomy: concepts, soil morphology and micromorphology. In: Ringrose-Voase AJ, Humphreys GS (eds) Soil micromorphology: studies in management and genesis. Developments in soil science, Vol. 22, Elsevier, Amsterdam, pp 117-131

White GN, Dixon JB (1996) Iron and manganese in nodules from a young Texas Vertisol. Soil Sci Soc Am J 60:1254-1262

Zhang M, Karathanasis D (1997) Characterization of iron-manganese concretions in Kentucky Alfisols with perched water tables. Clays Clay Miner 45:428-439

Figure captions

Figure 1. Typic nodules observed in the profile showing significant increase in their compactness with depth. (A) Typic nodule with gefuric fabric from the layer of 20-40 cm. Strongly diffuse edges, patchy cementation sometimes with collomorph structure (A1), irregular shape and large cracks are characteristic. (B) Typic nodule with forming outer coating band from the layer of 20-40 cm. Relatively compact but incomplete outer coating band with cementing material forming micro-bands and coatings (B1), as well as loosely stacked internal parts are characteristic. (C) Typic nodule with porphyric-like fabric and with a complete outer coating band (C1) from the layer of 60-90 cm. Rounded shape, diffuse edges, as well as vughy microstructure in their interior are characteristic (C1).

Figure 2. Concentric nodules observed in the profile. (A) Concentric nodule composed of numerous thin concentric bands from the layer of 60-90 cm. Less rounded shape, strongly diffuse edges, large voids and cracks settling circularly and interior impregnated weakly are characteristic. Their outer coating band can be partly lost as suggested by micro-bands reaching the surface (A1). (B) Compact concentric nodule with a few thick concentric bands from the layer of 90-120 cm. Rounded shape, slightly diffuse edges and compact interior with significantly different micro-fabric compared to that of their outer coating band (B1) are characteristic. (C) Geode-like concentric nodule from the layer of 60-90 cm. Nearly rounded shape, sharp edges, outer coating band almost lost (C1), one large internal band with several micro-band and a large void in their interior are characteristic. Where the outer band is lost, thin coating composed of silicates is present (C2).

Figure 3. Results of micro-chemical analyses of a typic nodule with gefuric fabric. (A) Backscattered electron images. Point analyses show that "clear" Mn oxides may appear even at the edge of such nodule, the close association of silicates and oxides (A1), as well as the dominance of Mn in the nodules interior (A2) (B) Elemental map and line-scan analysis. Fe shows patchy whereas Mn shows rather homogeneous distribution (B1). However, slight enrichment at the edges is suggested for both metals (B2). Characteristic EDS spectra from point analyses are also shown (A3).

Figure 4. Results of micro-chemical analyses of a typic nodule with porphyric fabric. (A) Backscattered electron image. Point analyses show that the outer part of the coating band is free of Mn, whereas this metal is present in its inner parts even as "clear" Mn oxides (A1). The dominance of Mn in such nodules' interior was also found (A2) (B) Elemental map and line-scan analysis. Separation of Fe and Mn is conspicuous here as Fe enrich at the edges whereas Mn in the interior of such nodules (B1 and B2). Characteristic EDS spectra from point analyses are also shown (A3).

Figure 5. Results of micro-chemical analyses of concentric nodules from different depth. (A) Backscattered electron image of a concentric nodule with large number of bands from the layer of 60-90 cm. Leaching of Mn from the outer parts of the coating band was observed (A1), whereas dominance of Mn within this band also decreases due to the gradual impregnation by Fe oxides (A2). Line scan analyses showed the Fe enrichment at the nodules' edges and development of inner bands with alternating Fe and Mn enrichment (A4). (B) Backscattered electron image of a concentric nodule with small number of bands from the layer of 120-150 cm. More intense leaching of Mn from the nodules' surface (B1) and its displacement by Fe in their interior than in shallower depth was observed (B2). Line scan analyses showed the marked separation of Fe and Mn both on outer and inner bands (B4). Characteristic EDS spectra from point analyses are also shown (A3, B3).

Figure 6. Results of micro-chemical analyses of concentric nodules with geode-like structure. Backscattered electron image shows the complete loss of the outer coating band (A). The thick, compact inner band exhibits the periodic increase of Fe/Mn ratio outwards (A1, A2). Elemental map (B1) and line-scan analyses (B2) showed the dominance of Fe in the internal bands and the marked separation of Fe and Mn.

Figure 1

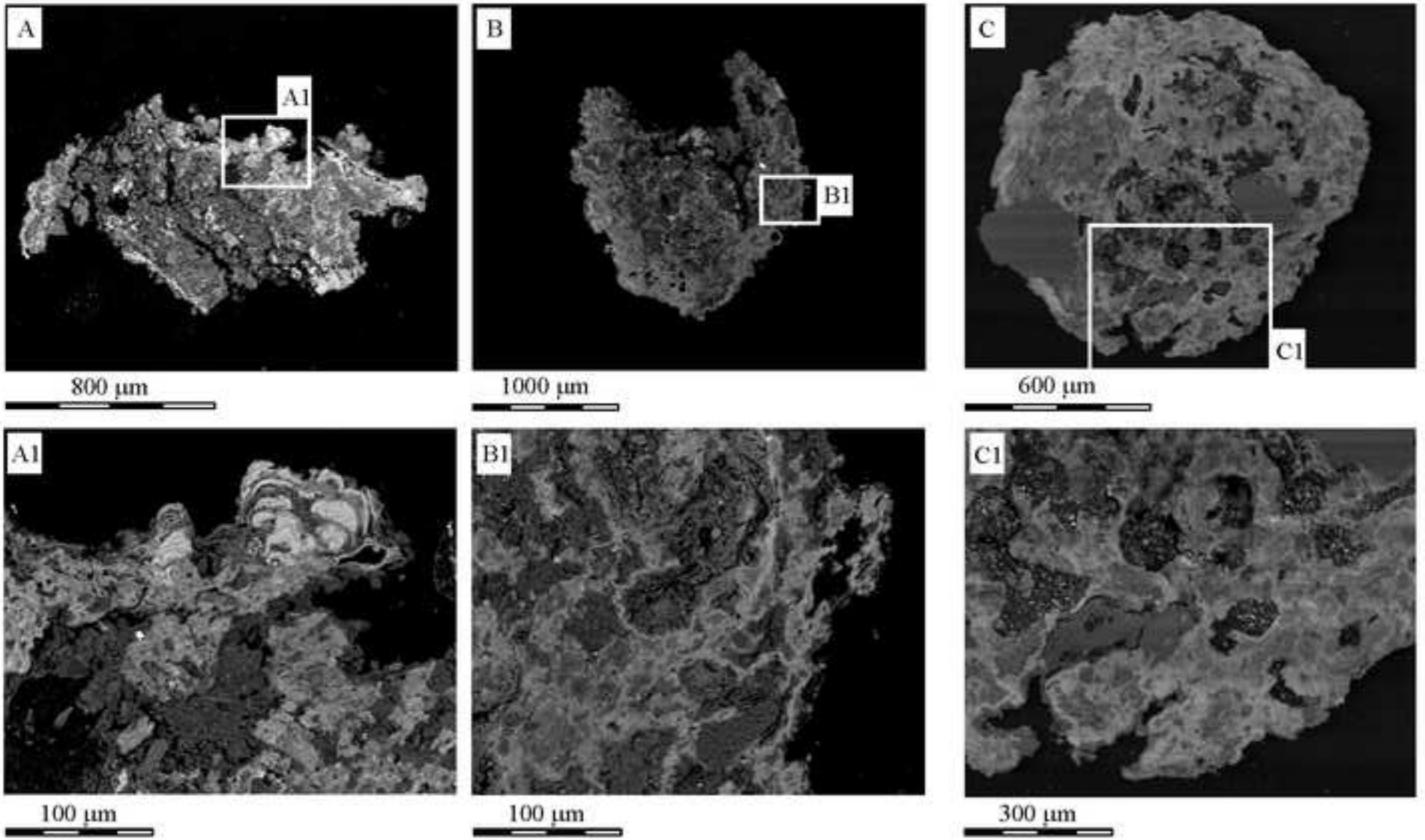

Figure 2

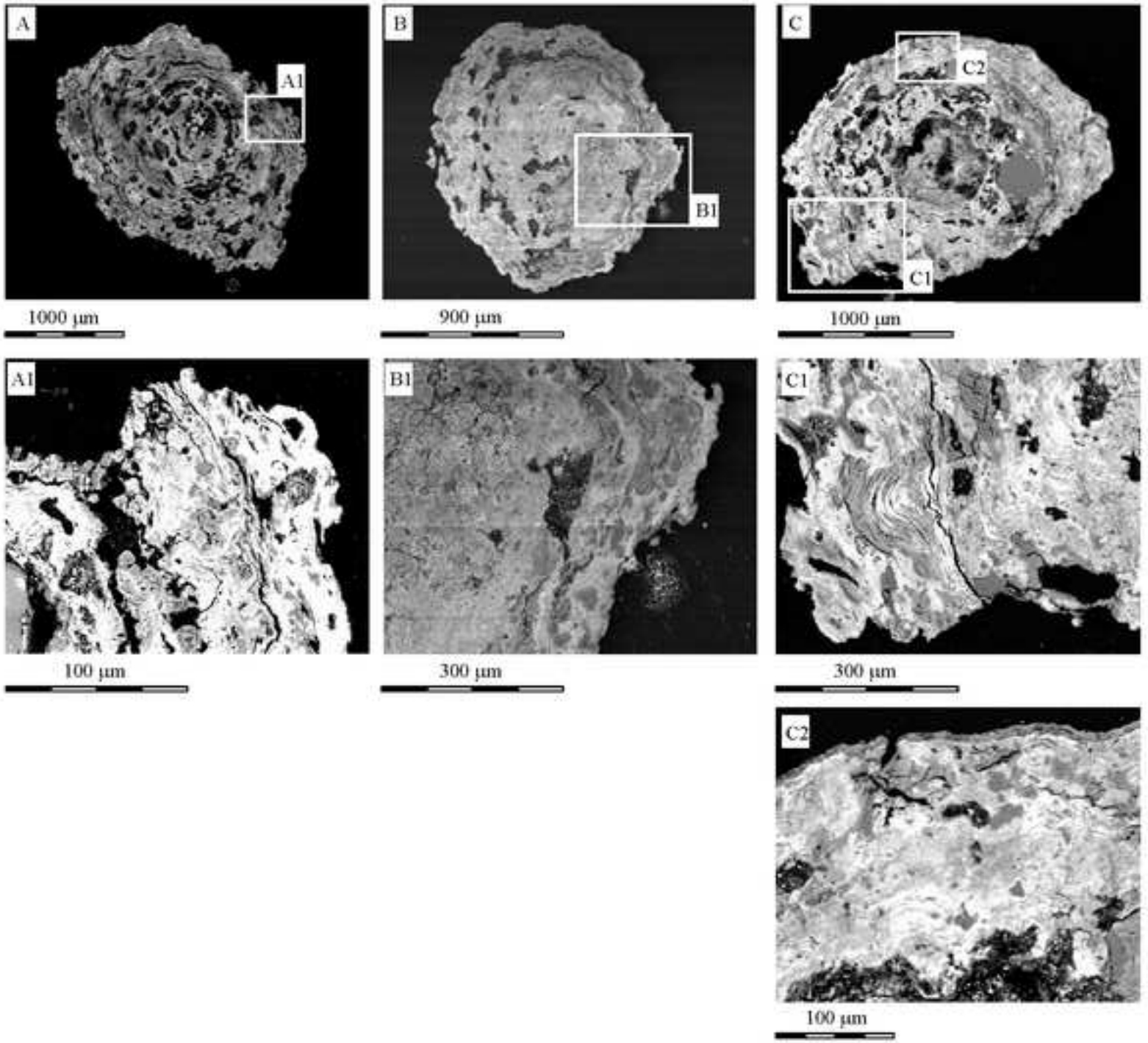
A
A1
1000 μm
B
B1
900 μm
C
C2
C1
1000 μm
A1
100 μm
B1
300 μm
C1
300 μm
C2
100 μm

Figure 3

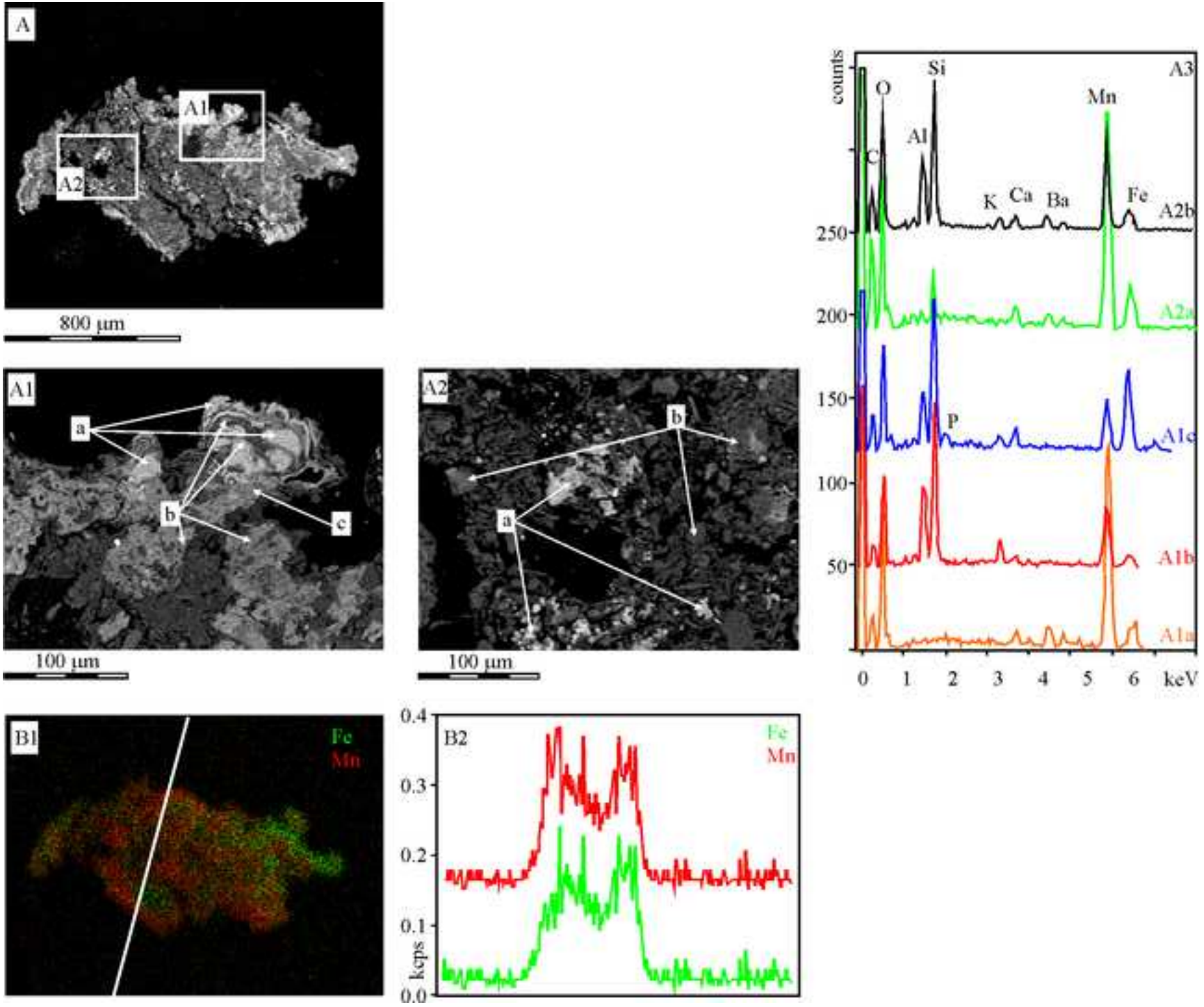
A
A1
A2
800 μm
A1
a
b
c
100 μm
A2
a
b
100 μm
counts
A3
O
Si
Mn
Al
C
K
Ca
Ba
Fe
A2b
A2a
A1c
P
A1b
A1a
250
200
150
100
50
0
1
2
3
4
5
6
keV
B1
Fe
Mn
B2
Fe
Mn
0.4
0.3
0.2
0.1
0.0
kcps

Figure 4

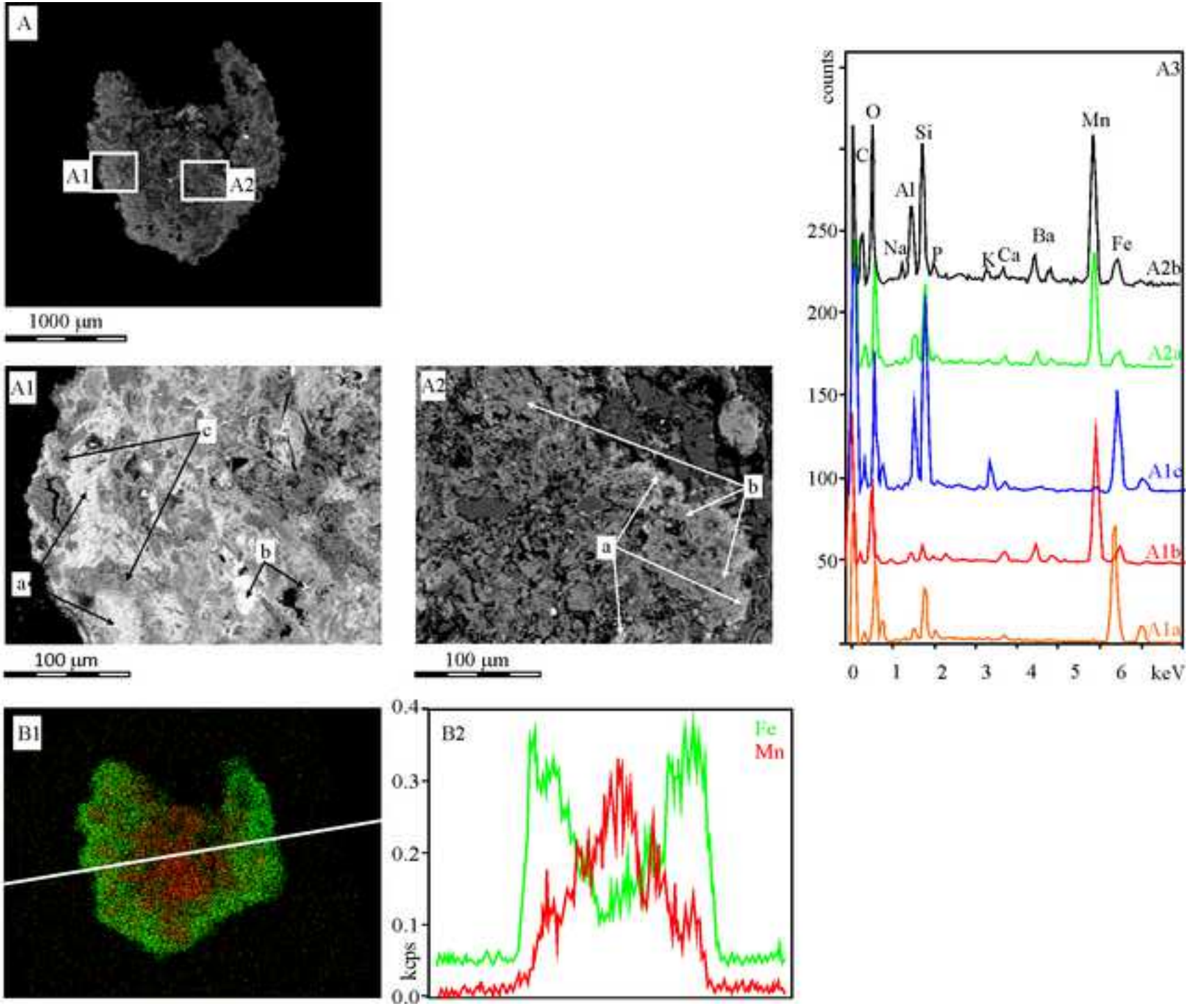
A
A1
A2
1000 μm
A1
c
b
a
100 μm
A2
b
a
100 μm
A3
counts
O
C
Si
Mn
Al
Na
P
K
Ca
Ba
Fe
A2b
A2a
A1c
A1b
A1a
250
200
150
100
50
0 1 2 3 4 5 6 keV
B1
B2
Fe
Mn
0.4
0.3
0.2
0.1
0.0
kcps

Figure 5

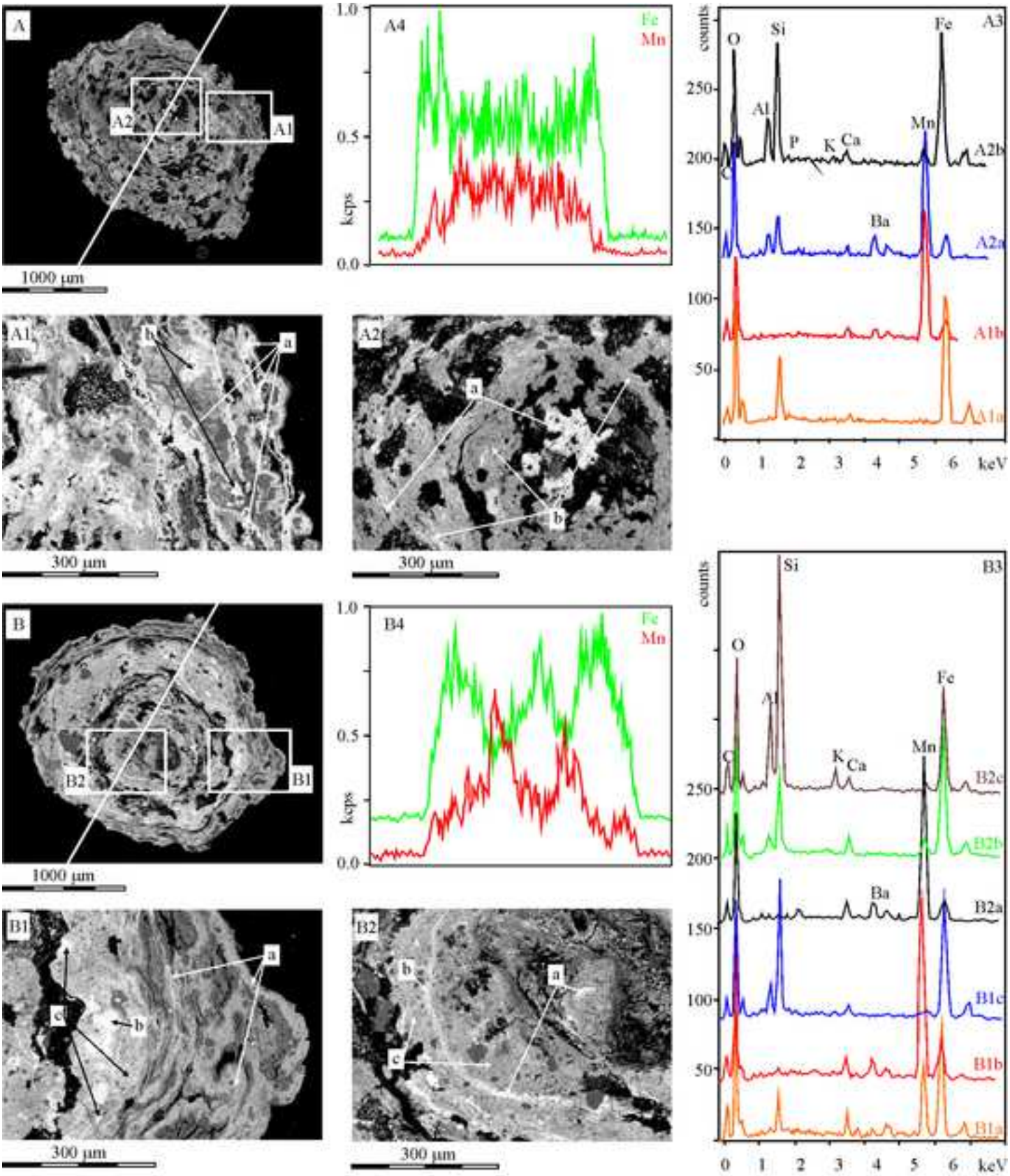
A
A2
A1
1000 µm
A4
Fe
Mn
1.0
0.5
0.0
kcps
A3
counts
O
Si
Al
P
K
Ca
Fe
Mn
Ba
A2b
A2a
A1b
A1a
250
200
150
100
50
0 1 2 3 4 5 6 keV
A1
b
a
300 µm
A2
a
b
300 µm
B
B2
B1
1000 µm
B4
Fe
Mn
1.0
0.5
0.0
kcps
B3
counts
O
Si
Fe
Mn
K
Ca
Ba
B2c
B2b
B2a
B1c
B1b
B1a
250
200
150
100
50
0 1 2 3 4 5 6 keV
B1
a
b
c
300 µm
B2
b
a
c
300 µm

Figure 6

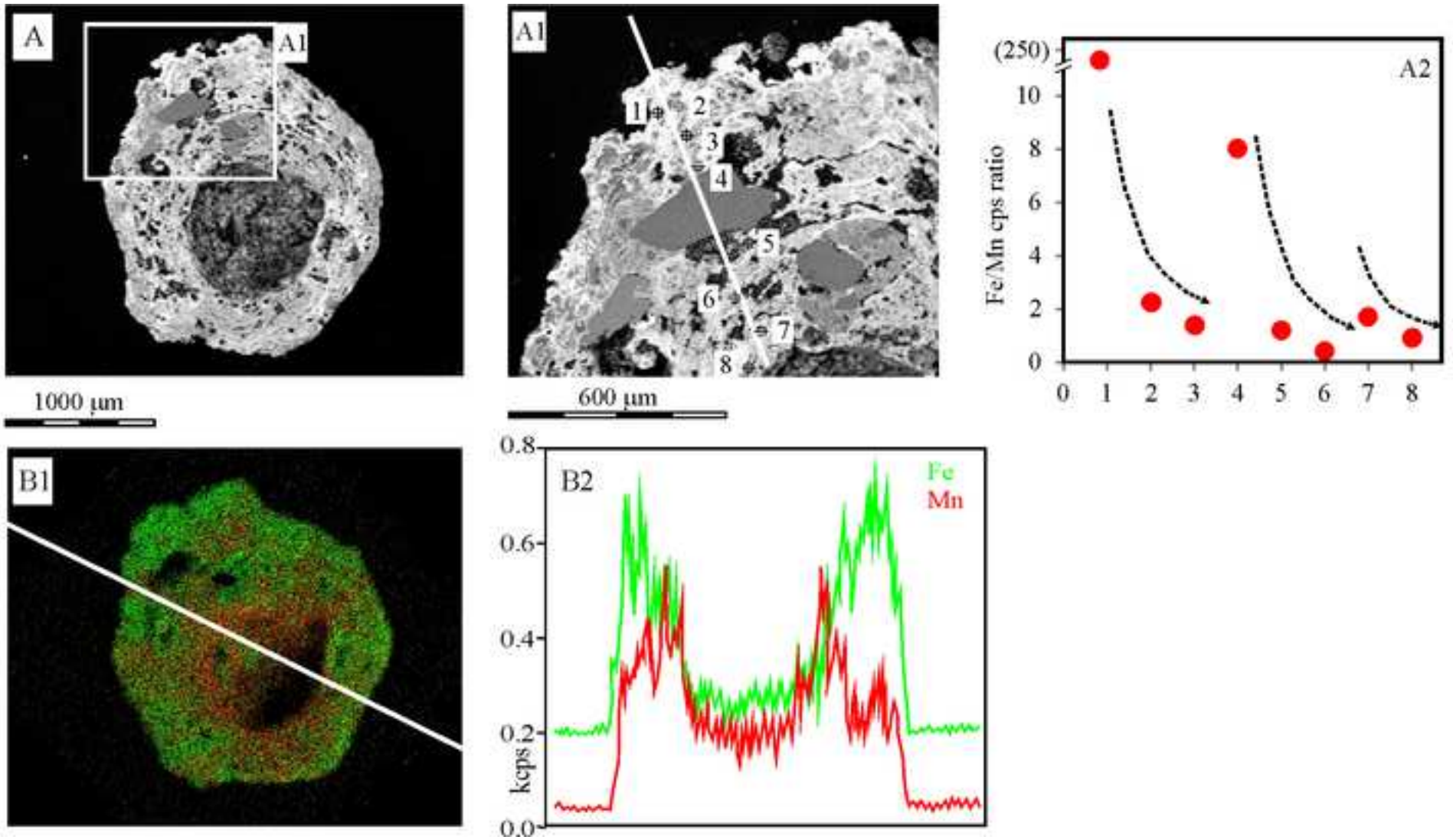
A
A1
1000 µm
A1
1
2
3
4
5
6
7
8
600 µm
(250)
10
8
6
4
2
0
Fe/Mn cps ratio
A2
0 1 2 3 4 5 6 7 8
B1
B2
Fe
Mn
0.8
0.6
0.4
0.2
0.0
kcps

Table 1. Some physico-chemical properties of the studied soil profile.

Depth (cm)	pH (H_2O)	TOC (%)	Loam (g/kg)	Clay (g/kg)	Fe_t (%)	Mn_t (mg/kg)	Fe_d/Fe_t	Fe_o/Fe_t	Fe_o/Fe_d	Mn_d/Mn_t	Mn_o/Mn_t	Mn_o/Mn_d
0-20	6.39	3.14	323	644	5.17 ± 0.02	910 ± 29						
20-40	6.68	1.55	327	628	5.25 ± 0.01	1148 ± 28	0.30	0.32	1.09	0.87	0.96	1.10
40-60	7.16	1.41	249	712	5.41 ± 0.03	939 ± 22						
60-90	7.46	0.98	196	699	5.39 ± 0.03	1212 ± 50	0.19	0.22	1.17	0.66	0.75	1.14
90-120	7.95	0.47	215	710	5.26 ± 0.02	1329 ± 15						
120-150	7.78	0.29	219	676	5.05 ± 0.07	1529 ± 50	0.16	0.17	1.04	0.77	0.79	1.04
150-180	7.91	0.17	162	609	4.39 ± 0.06	1297 ±22						
180-230	7.67	0.21	147	713	5.94 ± 0.02	549 ± 10	0.17	0.14	0.81	0.35	0.39	1.11
230-250	7.7	0.22	320	554	5.09 ± 0.05	333 ± 14						

t = total, d = dithionite-extractable, o = oxalate-extractable